

Analysis and Design of Spare Strategy for Large-Scale Satellite Constellation Using Markov Chain

Seungyeop Han^{*} and Zachary Grieser[†]
Georgia Institute of Technology, Atlanta, Georgia, 30332

Shoji Yoshikawa[‡], Takumi Noro[§], and Takumi Suda[¶]
Mitsubishi Electric Corporation, Amagasaki 661-8861, Japan

Koki Ho^{||}
Georgia Institute of Technology, Atlanta, Georgia, 30332

This paper presents a method for analyzing and designing an optimal spare-management policy in large-scale satellite constellations using a Markov chain model. To capture the stochastic nature of satellite failures and launch vehicle lead times, we adopt Markov chains to model both failure and replenishment processes. We reinvestigate an indirect spare strategy, modeled as a multi-echelon periodic-review reorder-point/order-quantity policy, in which spares are first delivered to parking orbits and then transferred to constellation planes. The stock levels in constellation and parking orbits are each modeled as independent Markov chains, and a fixed-point iteration yields a consistent joint stationary solution that describes the strategy's average behavior. This approach accurately captures the stochastic interplay within a multi-echelon model driven by orbital mechanics, avoiding the aggregation assumptions of prior works and remaining valid across a wider operating domain. Building on this fast, accurate analysis, we formulate an optimization problem and solve it via a genetic algorithm. Finally, we demonstrate the practical value of both the analysis method and the optimization framework in a real-world mega-constellation case study.

Nomenclature

τ_{mc}	=	Time step of the discrete-time Markov process, in days
λ_{sat}	=	Failure rate of a satellite, in failures per unit time

This paper is a substantially revised version of a portion of Paper AAS 24-164 presented at 2024 AAS/AIAA Astrodynamics Specialist Conference, Broomfield, CO, August 11-15, 2024.

^{*}Ph.D. Candidate, Daniel Guggenheim School of Aerospace Engineering

[†]Ph.D. Student, Daniel Guggenheim School of Aerospace Engineering

[‡]Chief Expert, Advanced Technology R&D Center, Mitsubishi Electric Corporation

[§]Researcher, Advanced Technology R&D Center, Mitsubishi Electric Corporation

[¶]Head Researcher, Advanced Technology R&D Center, Mitsubishi Electric Corporation

^{||}Dutton-Ducoffe Professor, Associate Professor, Daniel Guggenheim School of Aerospace Engineering, AIAA Senior Member, kokiho@gatech.edu
(Corresponding Author)

μ_{lv}	=	Mean interval between launches, in days
τ_{lv}	=	Constant launch order processing time, in days
τ_c/τ_p	=	RAAN alignment period from the perspective of in-plane/parking orbits
q_c/q_p	=	Replenishment quantity for in-plane/parking spares
r_c/r_p	=	Reorder point for in-plane/parking spares
N_{sat_c}/N_{sat_p}	=	Maximum in-plane/parking state level including operational and spare satellites
\bar{N}_{sat}	=	Nominal number of operational satellites per in-plane orbit
N_{orbit_c}/N_{orbit_p}	=	Number of in-plane (constellation)/parking orbital planes
P_{f_c}/P_{f_p}	=	Failure transition matrix for in-plane/parking states per review period
P_{q_c}/P_{q_p}	=	q -unit replenishment transition matrix for in-plane/parking states
π^{q_c}/π^{q_p}	=	Expected in-plane/parking state distribution immediately after q -unit replenishment
π^{r_c}/π^{r_p}	=	Expected in-plane/parking state distribution at the r -reorder point
π^{io_c}/π^{io_p}	=	Expected in-plane/parking state distribution during the inter-order (IO) period
π^{lt_c}/π^{lt_p}	=	Expected in-plane/parking state distribution during the lead-time (LT) period
π^{rc_c}/π^{rc_p}	=	Expected in-plane/parking state distribution over the full replenishment cycle (RC)

I. Introduction

THE satellite constellation is a coordinated group of satellites that together enable continuous global coverage. Constellations with thousands of satellites are becoming central to space-based communication infrastructure. Starlink has deployed over 9,000 satellites as of 2025 and plans to expand to more than 42,000 [1, 2]. Amazon's Project Kuiper began launching in 2025 and targets 3,236 satellites [3]. OneWeb, now under Eutelsat, has completed its initial deployment of 648 satellites and is planning expansion [4]. China's Guowang network is expected to include about 13,000 satellites and has already begun initial deployment [5]. These systems rely on advanced constellation architecture, frequency coordination, and inter-satellite communication, with a comparative analysis of their designs provided by Pachler et al. [6].

Over time, satellite failures reduce operational capacity and degrade constellation performance. To maintain service, an effective population management strategy is required. Two representative approaches are spare deployment and on-orbit servicing. The former inserts a spare satellite to replace a failed one [7], while the latter uses a servicer to repair the failed satellite [8]. Spare deployment is generally more suitable for mega-constellations with small, low-cost satellites, whereas servicing is more appropriate for smaller systems with high-value assets. In the context of low Earth orbit (LEO) mega-constellations, launching replacement satellites is widely regarded as more cost-effective than performing on-orbit repairs. This is driven by several factors: declining launch costs [9], economies of scale from mass

production, and the high expense of designing satellites to be serviceable. Additionally, small satellites tend to have higher failure rates due to limited testing and lack of redundancy [10], further reinforcing the need for rapid spare deployment. These trends motivate the study of optimal spare-management strategies, which is the focus of this paper.

Early work on spare deployment modeled satellite replenishment using an (s, S) inventory framework with exponential lead times, establishing a probabilistic basis for maintaining constellation performance [11]. Subsequent research analyzed various spare deployment strategies—including in-orbit, parking orbit, and ground-based options—across different phases of the constellation life cycle [7]. Discrete-time Markov decision processes were later applied to determine cost-optimal satellite replacement policies over finite planning horizons [12]. A more scalable formulation for mega-constellations was introduced through a multi-echelon reorder-point/order-quantity policy, commonly referred to as the (s, Q) inventory model or the (r, q) model, that considers parking orbits as intermediate warehouses between the ground and constellation planes [13].

Beyond inventory modeling, other studies have explored resilience and value-based assessment. A value model was developed to examine trade-offs between satellite reliability and system attributes such as cost or mass [14]. A quantitative resilience framework was proposed, incorporating robustness and recovery metrics to support mission-driven constellation optimization [15]. Resilience under solar weather radiation was also analyzed using a time-based simulation approach that evaluated reconstitution strategies and highlighted the influence of manufacturing and launch timelines on system performance [16].

Building on previous work [17], this paper introduces a novel Markov-based methodology for analyzing spare management strategies. The approach employs Markov processes to represent state transitions and analyze long-term behavior through stationary state distributions. The framework incorporates key physical realities often simplified in other models, such as the non-negativity of physical stock and state-dependent failure rates. The central contribution is the high-fidelity modeling of the multi-echelon replenishment dynamics. Unlike prior works that use aggregation assumptions, our approach models the stochastic interplay between the probability distribution of in-plane demand and that of parking orbit spare availability, a dynamic physically constrained by the periodic lead times from orbital mechanics. By computing the full state probability distribution, a step often intractable in prior analytical models, the framework enables a rigorous analysis of operational costs and constellation availability. We demonstrate the framework on a real-world mega-constellation case study.

The remainder of the paper is organized as follows. Section II introduces the modeling preliminaries. Section III presents the proposed analytical method for evaluating the indirect resupply strategy. Section IV applies this method to assess system performance. Section V validates the model through comparison with Monte Carlo simulations, and Section VI illustrates its application in a design optimization context. Finally, Section VII concludes the paper and suggests directions for future research.

II. Preliminaries

A. Spare Management Policy

1. Indirect Resupply Strategies

The indirect strategy uses a large launch vehicle (LV) to deliver spares to a parking orbit, from which they are transferred to the in constellation orbit via RAAN drift. Although this method benefits from batch discounts and lower launch cost, the RAAN drift introduces a longer replenishment delay. By contrast, the direct strategy employs a small LV to replenish the in plane orbit immediately. The detailed explanation for the direct strategy can be found in the past work[17].

Figure 1 illustrates the indirect strategy. If a failure occurs, an in plane spare immediately replaces the failed satellite, and whenever the number of in-plane spares falls below a threshold, a batch of spares is transferred from one of the parking orbits. At the same time, if the number of parking spares falls below a second threshold, a ground resupply order is placed and the replacement arrives after the LV's lead time. To enable these transfers, spare satellites are grouped into transfer buses and launched in batches aboard the large LV, allowing spares to be delivered to multiple constellation planes as needed.

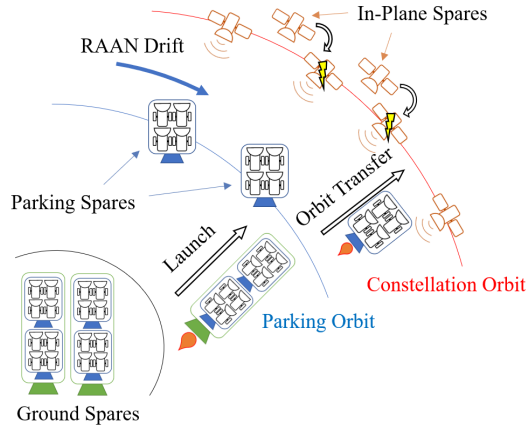


Fig. 1 Illustration of Indirect Spare Strategy

2. Inventory Management Policy

For the indirect method, both constellation and parking orbits use (r, q, τ) policies, also known as fixed review period (r, q) policies, but with different review periods and lead times. The in-plane review period is the time between successive alignments with a parking orbit, and its lead time is the fixed orbital transfer time. The parking review period is the time between alignments with a constellation orbit and its lead time comes from the lead time of heavy LV. At each review, if the stock level is $\leq r$ then an order of size q is placed; otherwise no order is made. Each order then arrives after its respective lead time with no orders between reviews.

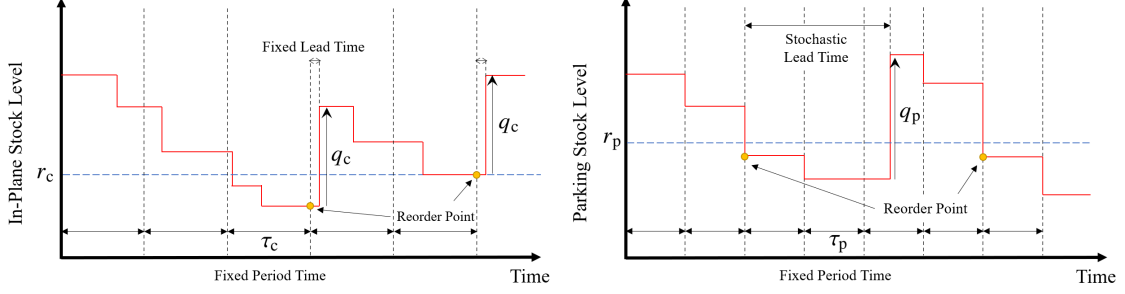


Fig. 2 Stock level profile of (a) constellation and (b) parking orbits under (r, q, τ) policy

B. Orbital Mechanics

1. Constellation Model

This research focuses on large-scale constellations in low Earth orbit (LEO), particularly the well-known Walker Delta pattern constellation[18]. This constellation comprises multiple circular constellation orbits with identical inclination angles. Additionally, the right ascension of the ascending node (RAAN) angle Ω of the constellation orbits is evenly distributed. In this configuration, there are a total of N_{orbit_c} constellation orbital planes (also referred as in-plane orbits), with nominal \bar{N}_{sat_c} satellites allocated to each constellation plane.

2. Parking Orbits

The parking orbits are temporary orbits where the batch of spares is first inserted for the indirect resupply strategy. There are a total of N_{orbit_p} parking orbits, and they are evenly distributed in RAAN. The parking orbits are assumed to have the same inclination angle as the constellation orbits but have different semi-major axes.

3. Orbital Maneuver

This research assumes that all orbit transfers are conducted using coplanar Hohmann transfers, and out-of-plane maneuvers are excluded due to their inefficiency in terms of delta-v. To facilitate these transfers, spare satellites are grouped with a transfer bus into a single batch. In a Hohmann transfer, the mass of fuel m_{fuel} needed for the transfer is computed as:

$$m_{\text{fuel}} = m_{\text{dry}}(e^{\Delta v/v_{\text{ex}}} - 1) \quad (1)$$

where m_{dry} is the dry mass of the spacecraft (e.g., set of spares and transfer bus), v_{ex} is the effective exhaust velocity and Δv is the velocity increment for the transfer. The Δv for this transfer can be calculated as follows:

$$\Delta v = \sqrt{\frac{\mu_{\oplus}}{a_p}} \left(\sqrt{\frac{2a_c}{a_p + a_c}} - 1 \right) + \sqrt{\frac{\mu_{\oplus}}{a_c}} \left(1 - \sqrt{\frac{2a_p}{a_p + a_c}} \right) \quad (2)$$

where μ_{\oplus} is the Earth's gravitational constant, and a_p and a_c ($a_c > a_p$) are the radii of initial (parking) and final (constellation) orbits, respectively.

The time of flight for a Hohmann transfer in LEO is typically on the order of a few hours. As this duration is negligible compared to the time horizon of the management policy, the maneuver is assumed to be instantaneous for modeling simplicity.

4. RAAN Drift

The LEO experiences non-negligible perturbations due to the oblateness of the Earth, resulting in the secular drift of the orbital plane. With an assumption of circular orbits, the RAAN drift rate of constellation and parking orbits are computed as:

$$\dot{\Omega}_c = -\frac{3}{2}J_2 \frac{R_{\oplus}^2}{a_c^2} \sqrt{\frac{\mu_{\oplus}}{a_c^3}} \cos i, \quad \dot{\Omega}_p = -\frac{3}{2}J_2 \frac{R_{\oplus}^2}{a_p^2} \sqrt{\frac{\mu_{\oplus}}{a_p^3}} \cos i \quad (3)$$

where a_c and a_p are the semi-major axis, i is the inclination of the constellation and parking orbit, R_{\oplus} is the Earth's radius, and J_2 is the second zonal harmonic coefficient of the Earth[19].

C. Markov Chain Model

We model the spare-satellite count as a discrete-time Markov chain. Let $X_k \in \{0, 1, \dots, N_{\text{sat}}\}$ be the number of satellites (including spares) at step k , and write the distribution

$$\pi_k = \left[\mathbb{P}(X_k = N_{\text{sat}}) \quad \mathbb{P}(X_k = N_{\text{sat}} - 1) \quad \dots \quad \mathbb{P}(X_k = 0) \right]^{\top}, \quad \pi_k(i) = \mathbb{P}(X_k = i) \quad (4)$$

Assuming a time-homogeneous transition matrix $P \in \mathbb{R}^{(N_{\text{sat}}+1) \times (N_{\text{sat}}+1)}$ with entries $P_{ij} = \mathbb{P}(X_{k+1} = i \mid X_k = j)$, the chain evolves by $\pi_{k+1} = P \pi_k$. Under the usual ergodicity conditions (e.g. P irreducible and aperiodic), the Markov Chain has a unique π satisfying

$$\pi = P\pi \quad (5)$$

and it gives the long-run fraction of time the chain spends in each state[20]. In our spare-management model, failures (state decreases) and replenishment (state increases) guarantee these conditions.

D. Probabilistic Model

1. Satellite Failure Probability Distribution

Satellite failures are modeled as a Poisson process (i.e. exponential interarrival times), and spare satellites are assumed not to fail. Although more accurate lifetime laws (e.g. Weibull or bathtub models) exist [21], the assumption of immediate failure replacement makes the Poisson model reasonable [13].

Let τ_{mc} denote the time step of the Markov process, and let λ_{sat} be the failure rate of an operational satellite per τ_{mc} . Then, the probability of observing k failures from n satellites (including spares) during τ_{mc} is given by:

$$\nu_{k,n} = \mathbb{P}(F = k | X = n) = \begin{cases} 0 & \text{if } k > \bar{N}_{\text{sat}} \\ \frac{(n\lambda_{\text{sat}})^k}{k!} e^{-n\lambda_{\text{sat}}} & \text{if } n \leq \bar{N}_{\text{sat}} \text{ and } k \leq \bar{N}_{\text{sat}} \\ \frac{(\bar{N}_{\text{sat}}\lambda_{\text{sat}})^k}{k!} e^{-\bar{N}_{\text{sat}}\lambda_{\text{sat}}} & \text{if } n > \bar{N}_{\text{sat}} \text{ and } k \leq \bar{N}_{\text{sat}} \end{cases} \quad (6)$$

where F is the number of failures, \bar{N}_{sat} is the nominal number of operational (non-spare) satellites. This formulation assumes immediate failure replacement and that spare satellites do not fail (i.e., $k > \bar{N}_{\text{sat}}$). When $n \leq \bar{N}_{\text{sat}}$, all satellites are operational, yielding a total failure rate of $n\lambda_{\text{sat}}$. When $n > \bar{N}_{\text{sat}}$, the number of operational satellites is fixed at \bar{N}_{sat} , making a total failure rate of $\bar{N}_{\text{sat}}\lambda_{\text{sat}}$, and excess satellites are treated as spares.

Additionally, let N_{satc} be the maximum number of satellites including spares in constellation orbits. Then the state transition matrix due to failure can be defined as:

$$P_f = \begin{bmatrix} \nu_{0,N_{\text{satc}}} & 0 & \cdots & 0 \\ \nu_{1,N_{\text{satc}}} & \nu_{0,N_{\text{satc}}-1} & \cdots & 0 \\ \vdots & \vdots & \ddots & \vdots \\ 1 - \sum_{k=0}^{N_{\text{satc}}} \nu_{k,N_{\text{satc}}} & 1 - \sum_{k=0}^{N_{\text{satc}}-1} \nu_{k,N_{\text{satc}}-1} & \cdots & \nu_{0,0} \end{bmatrix} \quad (7)$$

where $P_f \in \mathbb{R}^{(N_{\text{satc}}+1) \times (N_{\text{satc}}+1)}$. By construction, each column vector sums to one, and the matrix is lower triangular, clearly showing that multiplying by P_f always decrease the state level. In summary, if π is the in-plane state distribution, then $P_f \pi$ gives the distribution after a one-step failure.

2. LV Lead-Time Probability Distribution

The ground-resupply lead time is modeled as a shifted exponential distribution [13]: $T \sim \text{Exp}(\mu_{\text{lv}}) + \tau_{\text{lv}}$, and its probability density function is

$$f(T = t; \mu_{\text{lv}}, \tau_{\text{lv}}) = \begin{cases} \frac{1}{\mu_{\text{lv}}} e^{-(t-\tau_{\text{lv}})/\mu_{\text{lv}}} & t \geq \tau_{\text{lv}} \\ 0 & t < \tau_{\text{lv}} \end{cases} \quad (8)$$

where μ_{lv} is the mean of the exponential component and τ_{lv} is the fixed LV-processing delay. To simplify our discrete-time modeling, we choose τ_{mc} such that τ_{lv} is an integer multiple of τ_{mc} , i.e., $\tau_{\text{lv}} = k_{\text{lv}}\tau_{\text{mc}}$. Then the probability of having a

lead time between k and $k + 1$ time steps of τ_{mc} is computed as

$$\begin{aligned}\rho_{k+1} &= \mathbb{P}(k\tau_{\text{mc}} \leq T < (k+1)\tau_{\text{mc}}) \\ &= \begin{cases} e^{-k\tau_{\text{mc}}/\mu_{\text{lv}}} (1 - e^{-\tau_{\text{mc}}/\mu_{\text{lv}}}), & \text{if } k\tau_{\text{mc}} \geq \tau_{\text{lv}} \\ 0, & \text{otherwise} \end{cases}\end{aligned}\quad (9)$$

Note that each orbit is assumed to place at most one LV order at a time.

III. Modeling and Analysis of Spare Management Policy

The indirect resupply strategy is analyzed by solving the constellation-orbit and parking-orbit Markov chains independently, then enforcing consistency between them. Specifically, the constellation stock level depends on parking-orbit spare availability, while the parking stock level is driven by demand from the constellation orbits. In other words, the two chains are coupled through in-plane spares demand and parking spares availability. In the next subsection, we present each analysis step by step, and at the end of this section we show how to combine them.

Lastly, the subscripts $(\cdot)_{\text{c}}$ and $(\cdot)_{\text{p}}$ denote the constellation and parking orbits, respectively. The maximum number of satellites in constellation orbit is $N_{\text{sat}_{\text{c}}} = q_{\text{c}} + r_{\text{c}}$ in units of satellites, and the maximum number of parking spares is $N_{\text{sat}_{\text{p}}} = q_{\text{p}} + r_{\text{p}}$ in units of batches. That is, $\pi^{(\cdot)_{\text{c}}} \in \mathbb{R}^{N_{\text{sat}_{\text{c}}}+1}$ and $\pi^{(\cdot)_{\text{p}}} \in \mathbb{R}^{N_{\text{sat}_{\text{p}}}+1}$.

A. Repeating Structure of In-plane and Parking Orbits

As previously explained, the indirect strategy uses the relative RAAN drift between constellation and parking orbits to transfer spare satellites. Because the orbital planes are symmetrically distributed, each parking orbit and each constellation orbit align periodically. From a parking orbit's perspective, the interval between successive alignments with parking orbits is

$$\tau_{\text{c}} = \frac{2\pi}{N_{\text{orbit}_{\text{p}}} |\dot{\Omega}_{\text{c}} - \dot{\Omega}_{\text{p}}|} \quad (10)$$

Conversely, the interval for a parking orbit to align with successive constellation orbits is

$$\tau_{\text{p}} = \frac{2\pi}{N_{\text{orbit}_{\text{c}}} |\dot{\Omega}_{\text{c}} - \dot{\Omega}_{\text{p}}|} \quad (11)$$

With a proper selection of τ_{mc} or through rounding operations, τ_{c} and τ_{p} can be expressed as integer multiples of τ_{mc} as:

$$\tau_{\text{p}} = k_{\text{p}}\tau_{\text{mc}}, \quad \tau_{\text{c}} = k_{\text{c}}\tau_{\text{mc}} \quad k_{\text{p}}, k_{\text{c}} \in \mathbb{N} \quad (12)$$

B. Constellation Orbit Analysis Method

1. Replenishment Transition Matrix

Assume each parking-orbit stock X_p is independent and identically distributed, and let its state distribution just before a RAAN contact be known. We then define the parking-availability probability (see Section III.C.7) as

$$\kappa_j = \mathbb{P}(X_p \geq D_c = j|E) \quad (13)$$

where E denotes the RAAN contact event and D_c is the random variable for the demand in batches of size q_c from the in-plane orbit:

$$D_c = \begin{cases} \left\lceil \frac{r_c + 1 - X_c}{q_c} \right\rceil, & \text{if } X_c \leq r_c, \\ 0, & \text{if } X_c > r_c, \end{cases} \quad (14)$$

where $\lceil \cdot \rceil$ is the ceiling operator. For example, the demand is zero when the number of satellites exceeds r_c . On the other hand, if $X_c \leq r_c$, the demand corresponds to the number of batches required to raise the in-plane stock level above r_c . With these definitions, κ_j is the probability that at least j batches are available in the parking orbit when RAANs align.

Then the in-plane replenishment transition matrix becomes:

$$P_{q_c} = \begin{bmatrix} \kappa_0 I_{q_c} & \kappa_1 I_{q_c} & \kappa_2 I_{q_c} & \cdots \\ 0 & (\kappa_0 - \kappa_1) I_{q_c} & (\kappa_1 - \kappa_2) I_{q_c} & \cdots \\ 0 & 0 & (\kappa_0 - \kappa_1) I_{q_c} & \cdots \\ \vdots & \vdots & \vdots & \ddots \end{bmatrix}, \quad (15)$$

and $P_{q_c} \in \mathbb{R}^{(N_{\text{satc}}+1) \times (N_{\text{satc}}+1)}$. Each $q_c \times q_c$ block reflects the demand level and corresponding parking spare availability. For example, the first q_c entries of π (i.e., $r_c < X_c \leq N_{\text{satc}}$) require no replenishment so are multiplied by $\kappa_0 I_{q_c}$. The next q_c entries (i.e., $r_c - q_c < X_c \leq r_c$) has a demand of one batch. If the parking spare is available with κ_1 probability (i.e., (1,2) block), the stock level increase by q_c after replenishment. Otherwise, with probability $\kappa_0 - \kappa_1$ (i.e., (2,2) block), the state level remains unchanged. In summary, let π be the distribution right before receiving parking spares, then $P_{q_c} \pi$ is the distribution after receiving parking spares considering the parking availability.

2. Cycle Transition Matrix of Constellation Orbit

The replenishment cycle can be modeled as (r, q, τ) policy introduced in the Section II.A.2. Within the review period τ_c , the number of satellites will drop according to the P_f in Eq. (7) k_c times. Therefore, if the state distribution right after the replenishment (i.e., RAAN contact) was π^{q_c} then π^{r_c} , which is the distribution right before the review

period, becomes

$$\pi^{r_c} = P_{f_c} \pi^{q_c} = (P_f)^{k_c} \pi^{q_c}. \quad (16)$$

After having k_c number of unit steps, the system undergoes the replenishment process, completing the repeated structure as follows:

$$\pi^{q_c} = P_{q_c} P_{f_c} \pi^{q_c}, \quad \pi^{r_c} = P_{f_c} P_{q_c} \pi^{r_c}. \quad (17)$$

These cycle transition matrices $P_{q_c} P_{f_c}$ and $P_{f_c} P_{q_c}$ satisfy the necessary condition for the existence of a unique stationary distribution. Therefore, any numerical method applied will efficiently compute the stationary distributions π^{q_c} and π^{r_c} .

With this stationary distribution π^{q_c} , we can compute the average stock level during the replenishment cycle as:

$$\pi^{rc} = \frac{1}{k_c} \left(I + P_f + (P_f)^2 + \dots + (P_f)^{k_c-1} \right) \pi^{q_c}, \quad (18)$$

which represents the average state distribution over a τ_c period. For the case of in-plane analysis, the cycle period is same as review period as

$$\tau_{rc} = \tau_c = k_c \tau_{mc}. \quad (19)$$

3. Demand Distribution of Constellation Orbits to Parking Orbits

We compute the spare demand from constellation orbits over each review period τ_c , measured in units of batch size q_c . Just before RAAN contact (i.e., event E), the in-plane stock follows the distribution π^{r_c} , so the probability mass function (PMF) of the batch demand D_c at the contact moment is

$$\begin{aligned} \chi_j &= \mathbb{P}(D_c = j | E) \\ &= \sum_{k=j \cdot q_c}^{\min\{(j+1)q_c-1, N_{\text{sat}_c}\}} \pi^{r_c}(X_c = N_{\text{sat}_c} - k), \quad j = 0, 1, \dots \end{aligned} \quad (20)$$

Here χ_j is the probability that exactly j spare batches are required when the RAANs align, and this χ -vector then serves as input to the parking-orbit analysis. For example, if $r_c = 3$, $q_c = 2$ and $N_{\text{sat}_c} = 5$, then $\chi_0 = \pi^{r_c}(X_c = 4) + \pi^{r_c}(X_c = 5)$ since $D_c = 0$ when $X_c \in \{4, 5\}$.

C. Parking Orbit Analysis Method

1. Failure and Replenishment Transition Matrix of Parking Orbits

Assuming that spare satellites do not fail, the number of parking spares decreases only when they are transferred to the constellation orbits to meet demand*. Using the demand distribution from Eq. (20), the (demand-induced) failure

*If one wants to account for spare-satellite failures, multiplying by P_f at each time step yields the full transition matrix, as shown in the constellation orbit analysis.

transition matrix of the parking orbit at RAAN contact is

$$P_{f_p} = \begin{bmatrix} \chi_0 & 0 & \cdots & 0 \\ \chi_1 & \chi_0 & \cdots & 0 \\ \vdots & \vdots & \ddots & \vdots \\ 1 - \sum_{i=0}^{N_{\text{satp}}} \chi_i & 1 - \sum_{i=0}^{N_{\text{satp}}-1} \chi_i & \cdots & 1 \end{bmatrix}, \quad (21)$$

which has the same lower triangular structure as P_{f_p} in Eq. (7), with the failure probabilities ν replaced by the (demand-induced) failure probabilities χ . In summary, letting π be the parking state distribution before RAAN alignment, the product $P_{f_p}\pi$ gives the distribution immediately after alignment (i.e., after transferring the spares).

On the other hand, suppose a ground resupply has just been applied, and the stock level was $X_p = x$ for some $x \leq r_p$ immediately before replenishment. Then right after delivery it becomes $X_p = x + q_p$. Accordingly, we define the replenishment transition matrix P_{q_p} by

$$P_{q_p} = \left[\begin{array}{c|c} I_{q_p} & I_{r_p+1} \\ \hline \mathbf{0}_{(r_p+1) \times q_p} & \mathbf{0}_{q_p \times (r_p+1)} \end{array} \right], \quad (22)$$

and $P_{q_p} \in \mathbb{R}^{(N_{\text{satp}}+1) \times (N_{\text{satp}}+1)}$. Note that the upper-left block is chosen as I_{q_p} to keep P_{q_p} valid transition matrix. Since pre-delivery states with $X_p > r_p$ have zero probability (enforced by $C_{r_p}^-$), any other block would give the same end result. As in Eq. (15), $P_{q_p}\pi$ gives the distribution after receiving q_p spares, when π was the distribution immediately before replenishment.

Finally, to isolate probability mass above or below the reorder threshold r_p , define

$$C_{r_p}^+ = \begin{bmatrix} I_{N_{\text{satp}}-r_p} & \mathbf{0}_{(N_{\text{satp}}-r_p) \times (r_p+1)} \\ \mathbf{0}_{(r_p+1) \times (N_{\text{satp}}-r_p)} & \mathbf{0}_{r_p+1} \end{bmatrix}, \quad C_{r_p}^- = I_{N_{\text{satp}}} - C_{r_p}^+ \quad (23)$$

Then $C_{r_p}^+\pi$ gives the distribution for $X > r_p$ and $C_{r_p}^-\pi$ the distribution for $X \leq r_p$. These projections are key for deriving the failure and replenishment transition matrix.

2. Transition Matrix from Delivery to Reorder

This section derives the transition matrix from π^{q_p} to π^{r_p} . Within each review cycle of length k_p , a replenishment can arrive at any time step $i = 1, \dots, k_p$. Let $\pi_i^{q_p}$ denote the state distribution immediately after a delivery at step i . The

average post-delivery distribution is given by

$$\pi^{q_p} = \sum_{i=1}^{k_p} \eta_i \pi_i^{q_p}, \quad (24)$$

where η_i is the probability of delivery at time step i , whose expression is shown later in Eq. (26).

After a delivery at step i , the state distribution $\pi_i^{q_p}$ remains unchanged until the next review at step k_p , since no demands occur in between. At the review, part of the population $C_{r_p}^- P_{f_p} \pi_i^{q_p}$ triggers a reorder, while the rest $C_{r_p}^+ P_{f_p} \pi_i^{q_p}$ does not. After this review, the distribution again remains fixed for the next k_p steps, until the following review. At the second review, the non-reordering portion may reorder with distribution $C_{r_p}^- P_{f_p} C_{r_p}^+ P_{f_p} \pi_i^{q_p}$, or continue without reordering with distribution $C_{r_p}^+ P_{f_p} C_{r_p}^+ P_{f_p} \pi_i^{q_p}$ (see Fig. 3). Enumerating all such paths to the next reorder gives

$$\begin{aligned} \pi^{r_p} &= \sum_{i=1}^{k_p} \sum_{j=0}^{\infty} C_{r_p}^- P_{f_p} \left(C_{r_p}^+ P_{f_p} \right)^j \eta_i \pi_i^{q_p} \\ &= C_{r_p}^- P_{f_p} \left(I - C_{r_p}^+ P_{f_p} \right)^{-1} \sum_{i=1}^{k_p} \eta_i \pi_i^{q_p} \\ &= C_{r_p}^- P_{f_p} \left(I - C_{r_p}^+ P_{f_p} \right)^{-1} \pi^{q_p} \end{aligned} \quad (25)$$

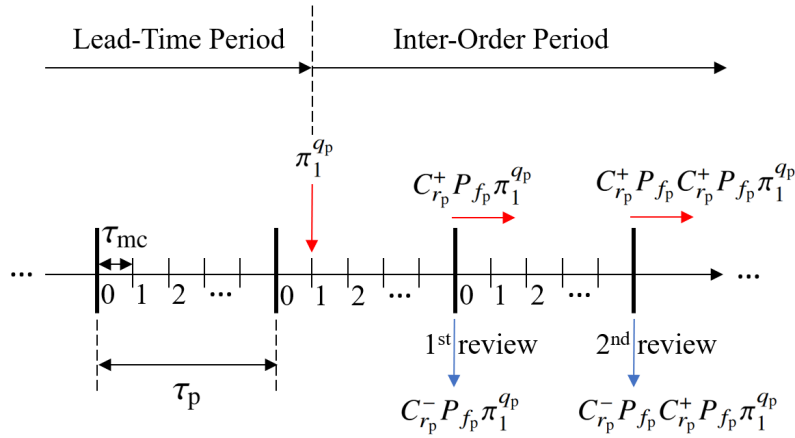


Fig. 3 Transition diagram during IO period when $\pi_1^{q_p}$ happens

3. Transition Matrix from Reorder to Delivery

This subsection derives the transition matrix from π^{r_p} to π^{q_p} . Under the (r, q, τ) policy, a reorder is placed only at the review point, which occurs at step 0. The probability that the replenishment arrives at step i of the j^{th} review period is given by ρ_{i+jk_p} , where ρ_l is the probability that the lead time equals l time steps.

To compute the marginal probability that a delivery occurs at step i (regardless of the review cycle index j), we sum

over all possible j :

$$\eta_i = \sum_{j=0}^{\infty} \rho_{i+jk_p} \text{ for } i = 1, \dots, k_p, \quad (26)$$

Given this, the distribution after a delivery at step i , defined as $\pi_i^{q_p}$, can be related to π^{r_p} by:

$$\eta_i \pi_i^{q_p} = \sum_{j=0}^{\infty} \rho_{i+jk_p} P_{q_p} \left(P_{f_p} \right)^j \pi^{r_p}. \quad (27)$$

where $\left(P_{f_p} \right)^j \pi^{r_p}$ gives the distribution after j reviews without delivery, and P_{q_p} applies the delivery transition when it occurs at step $i + jk_p$. For instance, deliveries that occur in the second review period ($j = 2$) contribute $P_{q_p} \left(P_{f_p} \right)^2 \pi^{r_p}$ with probability ρ_{i+2k_p} . Finally, the average post-delivery distribution is obtained by:

$$\begin{aligned} \pi^{q_p} &= \sum_{i=1}^{k_p} \eta_i \pi_i^{q_p} \\ &= \sum_{i=1}^{k_p} \sum_{j=0}^{\infty} \rho_{i+jk_p} P_{q_p} \left(P_{f_p} \right)^j \pi^{r_p} \\ &= \sum_{j=0}^{\infty} \sum_{i=0}^{k_p-1} \rho_{i+jk_p+1} P_{q_p} \left(P_{f_p} \right)^j \pi^{r_p}. \end{aligned} \quad (28)$$

Rearranging Eqs. (25) and (28) yields the cycle transition matrix, from which π^{q_p} and π^{r_p} are obtained. For a general lead-time model, an approximated summation must typically be used. However, for the assumed lead-time distribution in Eq. (9), an analytical expression for Eq. (28) can be derived, and the result is given in Eq. (49) in Appendix A.

4. Distribution during Inter-Order (IO) Period

This subsection derives the expression for $\pi_i^{\text{io}_p}$ in terms of π^{q_p} . Using the previously computed $\pi_i^{q_p}$, the distribution that avoids reordering for the next j consecutive review points is given by $\left(C_{r_p}^+ P_{f_p} \right)^j \pi_i^{q_p}$ (see Fig. 3). Since the state remains unchanged between reviews, the average state distribution during the IO period contributed by $\pi_i^{q_p}$ is proportional to:

$$\begin{aligned} \pi_i^{\text{io}_p} &\propto \left((k_p - i)I + \sum_{j=1}^{\infty} k_p \left(C_{r_p}^+ P_{f_p} \right)^j \right) \pi_i^{q_p} \\ &= \left((k_p - i)I + k_p C_{r_p}^+ P_{f_p} \left(I - C_{r_p}^+ P_{f_p} \right)^{-1} \right) \pi_i^{q_p} \end{aligned} \quad (29)$$

the first term $(k_p - i)$ reflects the remaining time steps before the first review epoch following delivery at step i . The second term accounts for the cumulative contribution from future review periods, each consisting of k_p steps.

Aggregating over all possible delivery steps i , weighted by their probabilities η_i , yields the final result as

$$\begin{aligned}\pi^{\text{io}_p} &= \frac{1}{k_{\text{io}_p}} \sum_{i=1}^{k_p} \eta_i \pi_i^{\text{io}_p} \\ &= \frac{1}{k_{\text{io}_p}} \left(\sum_{i=1}^{k_p} (k_p - i) \eta_i \pi_i^{q_p} + k_p C_{r_p}^+ P_{f_p} (I - C_{r_p}^+ P_{f_p})^{-1} \pi^{q_p} \right)\end{aligned}\quad (30)$$

where k_{io_p} is the normalization constant that ensures a valid state distribution. It also represents the expected IO period length in units of τ_{mc} , giving the time-converted interval as $\tau_{\text{io}_p} = k_{\text{io}_p} \tau_{\text{mc}}$.

5. Distribution during Lead-Time Period

This subsection derives the expression for π^{lt_p} in terms of π^{q_r} . The probability that the replenishment has not arrived by the ℓ^{th} time step is

$$\rho_\ell^c = 1 - \sum_{i=1}^{\ell} \rho_i, \quad \ell = 0, 1, \dots, \quad (31)$$

with $\rho_0^c = 1$. Therefore, the weighted distribution that is still awaiting delivery at the i^{th} time step of the j^{th} review period after the reorder moment is $\rho_{i+jk_p}^c (P_{f_p})^j \pi^{r_p}$. Then, the average distribution during the LT period becomes

$$\begin{aligned}\pi^{\text{lt}_p} &= \frac{1}{k_{\text{lt}_p}} \left[\left(\sum_{i=0}^{k_p-1} \rho_i^c \right) I + \left(\sum_{i=0}^{k_p-1} \rho_{i+k_p}^c \right) P_{f_p} + \dots \right] \pi^{r_p} \\ &= \frac{1}{k_{\text{lt}_p}} \sum_{j=0}^{\infty} \sum_{i=0}^{k_p-1} \rho_{i+jk_p}^c (P_{f_p})^j \pi^{r_p}\end{aligned}\quad (32)$$

where k_{lt_p} is the normalization constant and also represents the expected length of the LT period in time steps. As before, we can derive the analytical expression of Eq.(32) based on the assumed lead-time distribution in Eq.(9), and the resulting expression is given in Eq. (50) in Appendix A.

6. Distribution during Every Replenishment Cycle

Finally, since we have derived the state distributions during the IO and LT periods, along with their respective durations, the average state distribution in the parking orbit over a complete replenishment cycle under the indirect resupply policy is given by:

$$\pi^{\text{rc}_p} = \frac{k_{\text{io}_p}}{k_{\text{io}_p} + k_{\text{lt}_p}} \pi^{\text{io}_p} + \frac{k_{\text{lt}_p}}{k_{\text{io}_p} + k_{\text{lt}_p}} \pi^{\text{lt}_p}, \quad (33)$$

and the corresponding average duration of one replenishment cycle in the parking orbit is:

$$\tau_{\text{rc}_p} = \tau_{\text{io}_p} + \tau_{\text{lt}_p}. \quad (34)$$

7. Parking Spares Availability Distribution

From the parking-orbit analysis, we compute the availability distribution at the RAAN-contact event E . As stated in Eq.(13), we require the parking-spares distribution at the moment E occurs, which may fall within either the IO period or the LT period. Denoting the corresponding distribution for each case by $\pi^{\text{io}p|E}$ and $\pi^{\text{lt}p|E}$, whose closed-form expressions are derived in Eqs.(52) and (53) in the Appendix A, the average distribution conditioned on the event E during the entire period becomes:

$$\pi^{\text{rc}p|E} = \frac{k_{\text{io}p|E}}{k_{\text{io}p|E} + k_{\text{lt}p|E}} \pi^{\text{io}p|E} + \frac{k_{\text{lt}p|E}}{k_{\text{io}p|E} + k_{\text{lt}p|E}} \pi^{\text{lt}p|E} \quad (35)$$

where $k_{\text{io}p|E}$ and $k_{\text{lt}p|E}$ are the normalization constants of each distribution. Then, the parking availability probability in Eq. (13) can be computed as:

$$\kappa_j = \sum_{k=j}^{N_{\text{sat}p}} \pi^{\text{rc}p|E}(X_p = k) \quad (36)$$

D. Flow of Indirect Strategy Analysis

We split the coupled in-plane and parking-orbit analysis into two parts, as explained in the preceding subsections. Solving them independently yields inconsistent results, since they are coupled through ξ and κ , so we use fixed-point iteration, starting from 100 % parking availability($\kappa = 1$), to reach a consistent solution.

Although the analysis involves multiple steps, it takes only a few milliseconds on a standard computer. The detailed procedure for the indirect-resupply method is summarized in Table 1.

Algorithm 1 Fixed Point Iteration for the Indirect Strategy

Require: Constellation Configuration, Probability Model

```

 $\tau_c \leftarrow$  Eq. (10) and  $\tau_p \leftarrow$  Eq. (11)
 $P_f \leftarrow$  Eq. (7) and  $P_{f_c} \leftarrow$  Eq. (16)
 $P_{q_p} \leftarrow$  Eq. (22) and  $C_{r_p}^-, C_{r_p}^+ \leftarrow$  Eq. (23)
 $\kappa \leftarrow 1$  and  $k \leftarrow 0$ 
while  $|\kappa^{k+1} - \kappa^k| > \varepsilon$  or  $k < k^{\text{max}}$  do
     $P_{q_c} \leftarrow$  Eq. (15)
     $\pi^{q_c}, \pi^{r_c} \leftarrow$  Eq. (17) and  $\pi^{\text{rc}c} \leftarrow$  Eq. (18)
     $\chi \leftarrow$  Eq. (20) and  $P_{f_p} \leftarrow$  Eq. (21)
     $\pi^{q_p}, \pi^{r_p} \leftarrow$  Eqs. (25), (28)
     $\pi^{\text{io}p}, \pi^{\text{lt}p} \leftarrow$  Eqs. (30), (32) and  $\pi^{\text{rc}p} \leftarrow$  Eq. (33)
     $\pi^{\text{io}p|E}, \pi^{\text{lt}p|E} \leftarrow$  Eqs. (52), (53) and  $\pi^{\text{rc}p|E} \leftarrow$  Eq. (35)
     $\kappa \leftarrow$  Eq. (36) and  $k \leftarrow k + 1$ 
end while

```

IV. Performance Evaluation of Spare Management Policy

With the stationary solution $\pi^{rc(\cdot)}$ in hand, we can evaluate general performance metrics. The two most common metrics are operational cost and resilience, which trade off with each other.

A. Cost Model of Indirect Strategy

The total expected operating cost per unit time C_{total} is

$$C_{\text{total}} = C_{\text{build}} + C_{\text{hold}} + C_{\text{trans}} + C_{\text{launch}} \quad (37)$$

where C_{build} is the expected manufacturing cost of spares per unit time, C_{hold} is the expected holding cost per unit time, C_{trans} is the expected orbital maneuver cost per unit time, and C_{launch} is the expected launch cost per unit time.

Firstly, C_{build} is defined as:

$$C_{\text{build}} = \frac{1}{\tau_{\text{rcp}}} c_{\text{build}} N_{\text{orbitsp}} \cdot q_c \cdot q_p \quad (38)$$

where c_{build} is the manufacturing cost of a spare satellite. This reflects that $q_c \cdot q_p$ spares ($= q_p$ batches) are launched to each of the N_{orbitsp} parking orbits every τ_{rcp}

The holding cost represents the penalty for maintaining an excessive number of spares in orbit. It accounts for station-keeping costs, depreciation, and failure risk. It can be modeled as:

$$C_{\text{hold}} = c_{\text{holdc}} N_{\text{orbitc}} \sum_{i=\bar{N}_{\text{sat}}+1}^{N_{\text{satc}}} (i - \bar{N}_{\text{sat}}) \pi^{rc}(X_c = i) + c_{\text{holdp}} N_{\text{orbitp}} q_c \sum_{i=0}^{N_{\text{satp}}} i \pi^{rcp}(X_p = i) \quad (39)$$

where c_{holdc} and c_{holdp} are the holding cost of a spare satellite per unit time for constellation orbits and parking orbits, respectively.

The orbit transfer cost is modeled as follows:

$$C_{\text{trans}} = \frac{N_{\text{orbitc}}}{\tau_{\text{rc}} q_c} (c_{\text{fuel}} \cdot m_{\text{fuel}} + c_{\text{trans}}) \sum_{i=0}^{N_{\text{satc}}} i (\pi^{qc}(X_c = i) - \pi^{rc}(X_c = i)) \quad (40)$$

where c_{fuel} is the cost of fuel per unit mass, c_{trans} covers non-fuel transfer costs (e.g. bus build, transfer risk), and the fuel mass m_{fuel} is given by Eqs. (2) and (1), with $m_{\text{dry}} = q_c m_{\text{sat}} + m_{\text{bus}}$.

Lastly, the expected launch cost C_{launch} is modeled under two scenarios, depending on whether rideshare opportunities for parking orbits are available:

$$C_{\text{launch}} = \begin{cases} \frac{N_{\text{orbitp}}}{\tau_{\text{rcp}}} \min \{c_{\text{lv,unit}} m_{\text{total}}, c_{\text{lv,full}}\}, & \text{if rideshare available,} \\ \frac{N_{\text{orbitp}}}{\tau_{\text{rcp}}} c_{\text{lv,full}}, & \text{if rideshare unavailable.} \end{cases} \quad (41)$$

where $c_{lv,unit}$ is the launch cost to LEO per unit mass, $c_{lv,full}$ is the discounted price for reserving the full payload capacity of the launch vehicle, and $m_{total} = (m_{fuel} + m_{dry}) \cdot q_p$ is the total mass of the q_p batches. The minimum operator in the first case reflects the economic choice between paying the per-kilogram rate and purchasing a full-vehicle contract when rideshare missions to the target orbit are available. The second case assumes that rideshare is not offered for the desired orbit, so it must always purchase the full vehicle.

B. Resilience Model of Indirect Resupply Strategy

The proper resilience metric should capture both agility (how quickly the system recovers to nominal capacity) and robustness (the depth of capability loss when operating below nominal) [22, 23]. In practice, this is often measured by the area under the nominal-capacity line that is lost over time, i.e. the time-integral of the deficit. In our discrete-time Markov model this becomes the expected shortage S_c

$$S_c = \sum_{i=0}^{\bar{N}_{sat}} (\bar{N}_{sat} - i) \cdot \pi^{rc_c}(X_c = i), \quad (42)$$

which multiplies each deficit $\bar{N}_{sat} - i$ by the fraction of time spent in state i as $\pi^{rc_c}(X_c = i)$.

In a parking orbit there is no nominal capacity level, so the expected-shortage metric does not apply. Instead, we define resilience as the out-of-stock probability:

$$\mathbb{P}(X_p = 0) = \pi^{rc_p}(X_p = 0) \quad (43)$$

which is the long-run fraction of time the parking orbit has zero spares.

C. Optimization Problem for Indirect Resupply Strategy

There are multiple ways to formulate the optimization problem, but here we focus on minimizing the total operating cost of the spare policy while enforcing resilience and launch-vehicle constraints. The problem can be stated as

$$\begin{aligned} \min_x \quad & C_{total} \\ \text{s.t.} \quad & g_1 = S_c - \varepsilon_1 \leq 0 \\ & g_2 = \mathbb{P}(X_p = 0) - \varepsilon_2 \leq 0 \\ & g_3 = m_{total} - m_{payload} \leq 0 \\ & q_c, r_c, q_p, r_p, N_{orbit_p} \in \mathbb{Z}^+ \end{aligned} \quad (44)$$

where $x = (q_c, r_c, q_p, r_p, N_{orbit_p}, h_p)$, and ε_1 and ε_2 are user-defined thresholds. The g_3 constraint ensures that the total mass does not exceed the vehicle's maximum payload capacity $m_{payload}$. By solving this optimization problem, one can

estimate the approximate cost required to maintain the satellite constellation.

V. Numerical Validation of the Analysis Method

A. Numerical Validation Set-up

The analytical model developed above enables efficient evaluation of spare policies even for mega-scale constellations, but it relies on simplifying assumptions such as independent and identically distributed stock levels in both constellation and parking orbits. To validate the proposed method, we follow the approach introduced in [13].

When validating the model, we could directly compare histograms of simulated stock levels with $\pi^{\text{rc}(\cdot)}$, but summarizing those differences in a single metric is difficult. Instead, we compare the mean stock levels of in-plane and parking orbits, the expected shortage of the constellation orbit, and the out-of-stock probability of the parking orbit, which are key metrics for performance evaluation. The mean stock level is computed as

$$M_{(\cdot)} = \sum_{i=0}^{N_{\text{sat}(\cdot)}} i \cdot \pi^{\text{rc}(\cdot)}(X_{(\cdot)} = i). \quad (45)$$

Finally, we construct 100 unique test cases using Latin hypercube sampling over the parameters in Table 3, with fixed parameters given in Table 2. For each test case, we run a 20-year simulation 100 times and report the averaged statistics.

B. Numerical Validation Results

As noted in our earlier work [17], the proposed analysis can lose accuracy when the i.i.d. assumption for parking orbits breaks down. This occurs if parking spares are out of stock for extended periods, which typically happens when the satellite failure rate exceeds the replenishment capacity and disrupts the conventional saw-tooth stock profile. Consequently, the heuristic threshold $\mathbb{P}(X_p = 0) < 1/(N_{\text{sat}_p} + 1)$, derived from an even-distribution assumption, is used here to select valid cases for comparison.

The fidelity of the analytical framework is confirmed by the results summarized in Table 4, which show a 95th percentile error of less than 1% across all performance metrics. The minor deviations between the analytical and simulated results are attributed to the statistical noise inherent in the Monte Carlo method and the model's i.i.d. assumption for the parking orbits. It should be noted that the relative errors for M_p and S_c are larger than for M_c , which is a known effect of using relative error metrics on quantities with small nominal values. The overall validity of the method is further demonstrated in Fig. 4, which shows a close alignment of the probability distributions for a representative case near the maximum error level.

In terms of computational cost, the proposed method offers a significant advantage. The full Monte Carlo simulation required approximately several hours to complete each test case, whereas the analytical framework produced a solution in under a second using appropriate numerical techniques. The method is therefore both accurate and highly efficient,

making it suitable for use as the inner loop in an optimization process.

C. Numerical Validation Result

The main assumption of this research is that parking orbits are independent and identically distributed. This assumption may become invalid if parking spares are out of stock for an extended period, which can create stronger correlations between parking orbits. Such a situation arises when the failure rate exceeds the replenishment capacity of the launch vehicle, and it can be detected through the out-of-stock probability $\mathbb{P}(X_p = 0)$ defined in Eq. (43). In this study, we evaluated the accuracy of the method only for cases where $\mathbb{P}(X_p = 0) < \frac{1}{N_{\text{satp}} + 1}$.

The test results are summarized in Table 4. For error computation, relative error is used for M_c , M_p , and S_c , while absolute error is used for $\mathbb{P}(X_p = 0)$. The small observed discrepancies between the model and simulation results stem from a combination of the model's i.i.d. assumption and the statistical noise inherent in finite-duration Monte Carlo simulations. The higher relative errors reported for M_p and S_c compared to M_c are primarily an artifact of their small nominal values, a known characteristic of the relative error metric. Crucially, even with these combined effects, the 95th percentile error across all metrics remains below 1%, which confirms the high accuracy and practical value of the analytical model. Even in the worst cases, direct comparisons of the probability distributions show that the proposed method accurately captures system behavior. A representative case with near-maximum error across all four metrics is illustrated in Fig. 4.

Lastly, in terms of computational cost, the full simulation took more than several hours, whereas the proposed method required only a few milliseconds to compute each test case. This demonstrates that the proposed method is both accurate and efficient, making it suitable for use as an inner loop in the optimization process.

Table 2 Fixed simulation parameters

Parameter	Notation	Value	Unit
Markov time step	τ_{mc}	0.5	days
Constellation orbit altitude ($a_c - R_{\oplus}$)	h_c	1200	km
Inclination of orbit planes	i	50	deg
Number of constellation orbits	N_{orbit_c}	40	orbits
Nominal satellites per plane	\tilde{N}_{sat}	40	satellites

D. Comparison with Existing Method

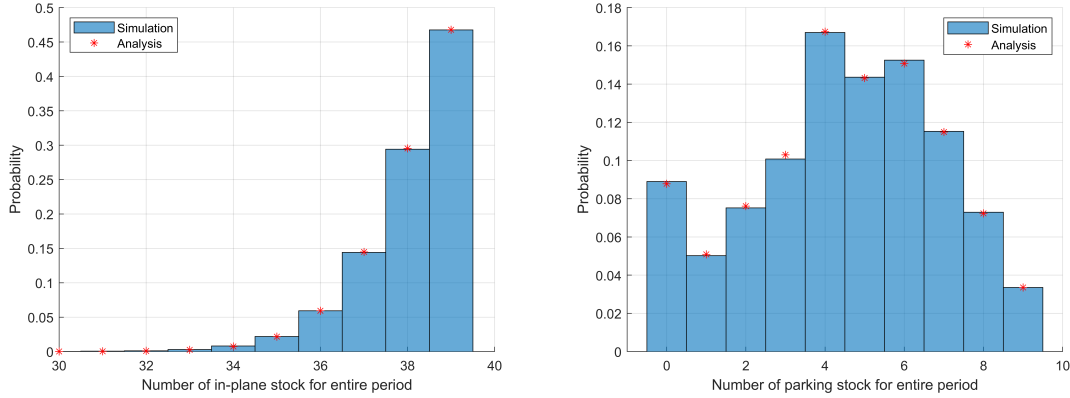
The previous work [13] assumes that the demand for parking spares follows a Poisson process and that the lead time from parking orbits to constellation orbits follows a uniform distribution, based on the assumption of a high order fill rate. Specifically, the lead time is defined as the duration from the moment $X_c \leq r_c$ to the next RAAN alignment with

Table 3 Bound of sampled simulation parameters

Parameter	Notation	Bounds	Unit
Satellite failure rate	λ_{sat}	[0.001, 0.5]	failures/satellite/year
Launch order processing time	τ_{lv}	[0, 60]	days
Mean exponential launch lead time	μ_{lv}	[5, 60]	days
Order size for in-plane spares	q_c	[1, 20]	satellites
Order size for parking spare batch	q_p	[1, 20]	batches
Reorder point for in-plane spares	r_c	$[\bar{N}_{\text{sat}} - 5, \bar{N}_{\text{sat}} + 5]$	batches
Reorder point for parking spare batch	r_p	[0, 10]	batches
Parking orbit altitude ($a_p - R_{\oplus}$)	h_p	[500, 1100]	km
Number of parking orbits	N_{orbit_p}	[1, 20]	orbits

Table 4 Error between proposed method and simulation results

Parameter	Mean	P95
Relative error of M_c	0.012 %	0.035 %
Relative error of M_p	0.172 %	0.432 %
Relative error of S_c	0.191 %	0.794 %
Absolute error of $\mathbb{P}(X_p = 0)$	0.006 p.p	0.019 p.p

**Fig. 4 Comparison results for the representative case of large error: (a) π^{rc_c} ; (b) π^{rc_p}**

the nearest parking orbit, and the following parameter is used for Poisson demand [13]:

$$\lambda_{\text{demand}} = \frac{N_{\text{orbit}_c} \bar{N}_{\text{sat}}}{q_c N_{\text{orbit}_p}} \lambda_{\text{sat}} \tau_c. \quad (46)$$

However, our simulations reveal significant deviations from these assumptions. Figure. 5 shows that the lead time distribution from simulation (blue histogram) is skewed and clearly non-uniform, a characteristic not captured by the uniform model (black line). Similarly, Fig. 6, demonstrates that the Poisson distribution (black circles) is a poor fit for the simulated spare demand.

These discrepancies persist even in near-ideal scenarios with low failure rates and high parking-spare availability, indicating a fundamental limitation in the prior model’s ability to represent the system’s stochastic interplay. In contrast, our proposed analysis (red line and circles) shows excellent agreement with the simulation data in both figures.

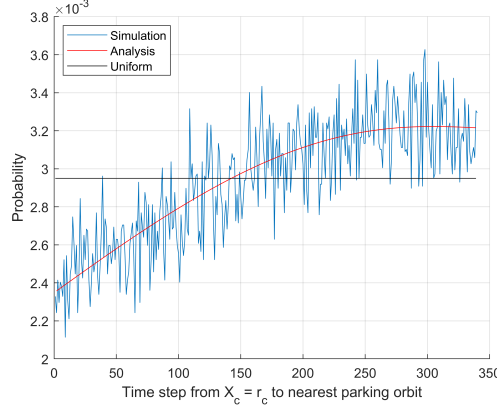


Fig. 5 The histogram of time from $X_c = r_c$ to align with closest parking orbit

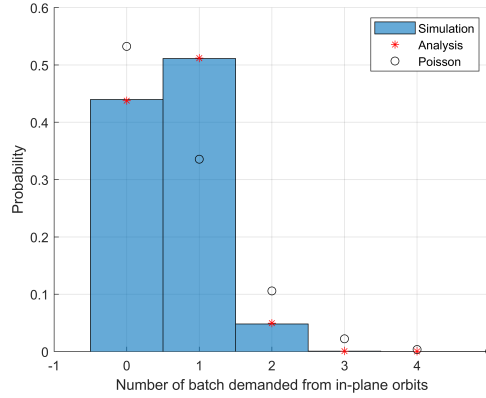


Fig. 6 The histogram of demand of in-plane spares at RAAN align of representative case

VI. Optimization of Spare Management Policy

One key application of the proposed analysis method is design optimization. An optimization problem can be formulated to guide early-phase spare strategy decisions, such as monthly replenishment needs or cost estimates. In this section, we optimize the indirect strategy using the formulation in Eq. (44) with real-world parameters. The resulting cost is then compared to that of the direct strategy. Since the direct strategy for constellation orbits is analytically equivalent to the indirect strategy for parking orbits under continuous review, Appendix B outlines how the direct results can be derived from the framework presented here. An alternative independent derivation of the direct strategy, as well as its more detailed discussion, can be found in [24].

For the direct strategy, we assume the use of a small launch vehicle, specifically Rocket Lab’s Electron, while

the indirect strategy employs a heavy launch vehicle, namely SpaceX’s Falcon 9, with launch costs referenced from [25, 26]. Although the lead time for both vehicles can, in principle, be as short as two days [27, 28], such estimates are optimistic and do not account for contract processing or shipping delays. To reflect a more realistic timeline, we adopt $(\mu_{lv}, \tau_{lv}) = (20, 20)$ days for Falcon 9 and $(10, 10)$ days for Electron, making the Falcon 9 lead time roughly twice as long. For Electron we assume $c_{lv,full} = 7.5$ M\$ and $m_{payload} = 300$ kg.

Regular rideshare opportunities are generally limited to low altitudes with common inclinations such as sun-synchronous or ISS orbits. Since our constellation orbit does not fall into this category, rideshare is not feasible for the direct strategy, and Electron with a full-vehicle contract is assumed instead. For the indirect strategy, Falcon 9 is considered for parking-orbit replenishment, as its unit cost is substantially lower than Electron and rideshare may be feasible at lower altitudes. Accordingly, we evaluate two indirect models: one with rideshare access and one without. The remaining parameters are summarized in Table 2 and Table 5.

Table 5 Parameters for the optimization

Parameter	Notation	Value	Unit
Satellite manufacturing cost	c_{build}	0.5	M\$/satellite
In-orbit spares annual holding cost	c_{hold_e}	0.5	M\$/satellite/year
Parking spares annual holding cost	c_{hold_p}	0.5	M\$/satellite/year
Launch cost per unit mass (Falcon 9)	$c_{lv,unit}$	6500	\$/kg
Discounted cost for full contract (Falcon 9)	$c_{lv,full}$	67	M\$
Payload launch maximum capacity (Falcon 9)	$m_{payload}$	18500	kg
Fuel cost per mass	c_{fuel}	0.001	M\$/kg
Non-fuel transfer cost	c_{trans}	0.5	M\$
Mass of satellite	m_{sat}	150	kg
Mass of transfer bus	m_{bus}	100	kg
Effective exhaust velocity	v_{ex}	2.16	km/s

A. Baseline Scenario

As a baseline scenario, we consider a moderate failure rate of $\lambda_{sat} = 0.05$, with resilience thresholds $\varepsilon_1 = 0.25$ for S_c and $\varepsilon_2 = 1/(N_{sat_p} + 1)$ for the out-of-stock probability. Optimization is performed using a genetic algorithm. For the indirect strategy, the optimal solution is $x^* = (4, 40, 23, 2, 1, 735)$ regardless of rideshare availability. In this case, using the full Falcon 9 contract minimizes cost, as the savings in launch cost outweigh the increase in holding cost from parking spares. The direct strategy, which has only two integer design variables (r, q) , yields $(q^*, r^*) = (2, 39)$.

As shown in Table 6, the indirect strategy achieves a 53% reduction in total cost, primarily due to the much lower launch cost per satellite enabled by Falcon 9. Although it incurs additional holding and transfer costs, these are offset by the launch savings. The build cost C_{build} remains similar between the two strategies because the same resilience requirement under the same failure rate leads to a similar number of spare satellites being produced. Lastly, the direct

strategy naturally avoids transfer operations, but due to the small design space, i.e., q and r , the S_c constraint is satisfied with an excessive margin.

This baseline case shows that, under realistic launch cost assumptions, the indirect strategy can achieve the required resilience at significantly lower cost than the direct strategy.

Table 6 Summary of results for representative scenarios.

Policy	C_{total} [M\$/day]	Detailed Costs [M\$/day]				Constraints	
		C_{build}	C_{hold}	C_{launch}	C_{trans}	S_c	$\mathbb{P}(X_p = 0)$
Direct(no-RS)	0.9547	0.1094	0.0246	0.8207	N/A	0.0591	N/A
Indirect(no-RS)	0.4479	0.1082	0.1507	0.1575	0.0316	0.2387	0.0286
Indirect(RS)	0.4479	0.1082	0.1507	0.1575	0.0316	0.2387	0.0286

Note: RS = rideshare available; no-RS = rideshare unavailable.

B. Sensitivity to failure rate

Satellite failure rates vary over time and depend on system scale. Smaller satellites generally exhibit higher failure rates than larger ones [29–31]. Since it is difficult to define a single representative value, we test a wide range of failure rates from 0.01 to 0.5 failures per year.

In this experiment, only the satellite failure rate is varied, while all other parameters are kept the same as in the baseline scenario. Figure 7 shows the total cost of each strategy and the relative savings of the indirect strategy (IS) compared to the direct strategy (DS). Higher values indicate greater cost reduction of IS over DS. IS is more cost efficient than DS across the entire failure rate range. At very low failure rates (around 0.01), relatively few spares are needed to satisfy the S_c constraint. In this case, rideshare can reduce cost, while full-contract launches provide little advantage because the additional holding cost offsets the savings. As the failure rate increases, more spares and more frequent launches are required. Since launch cost dominates the budget, the advantage of IS grows with failure rate. Overall, the use of heavy launch vehicles makes the indirect strategy cost effective across all tested cases.

VII. Conclusion

In this paper, we developed a Markov chain-based framework for the detailed analysis and design of an indirect spare management policy in large-scale constellations. We modeled in-plane and parking orbits as (r, q, τ) systems, solved their coupled stationary distributions via fixed-point iteration, and derived expressions for cost and resilience metrics. Building on this fast, accurate analysis, we formulated an optimization problem and solved it with a genetic algorithm to minimize total operating cost under resilience constraints. Using this framework, we compared the indirect strategy to the direct strategy and characterized its behavior through sensitivity analysis. Our results show that the indirect strategy is advantageous when it can leverage lower launch costs. Finally, this framework can be extended to other constellation

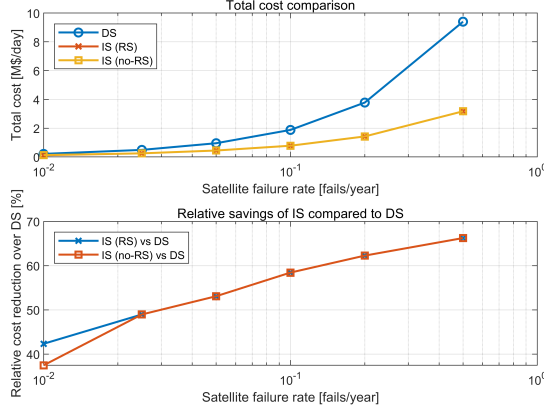


Fig. 7 Relative C_{total} savings of IS compared to the DS across different satellite failure rates.

configurations (e.g., asymmetric and heterogeneous) and alternative replenishment policies, which we will explore in future work.

Appendix A: Closed-Form Expressions for Eqs. (28), (32), and (35)

In this appendix, we derive the analytical expression using the explicit equation of the exponential lead time distribution.

Closed-Form Expression for Eq. (28)

In this work, we can derive a closed-form expression for Eq.(27) using the explicit lead-time probability formula from Eq.(9). Referring to Fig. 8, we define the following integers:

$$m_{lv} = \left\lfloor \frac{\tau_{lv}}{\tau_p} \right\rfloor, \quad k_{\text{left}} = k_{lv} - m_{lv}k_p, \quad k_{\text{right}} = (m_{lv} + 1)k_p - k_{lv} \quad (47)$$

where m_{lv} denotes the index of the first review period during which a delivery can occur, and k_{left} indicates the time step at which the fixed processing delay is completed (i.e., when ρ_j first becomes nonzero). Here, $\lfloor \cdot \rfloor$ is the floor operator. Since $\tau_{(\cdot)} = k_{(\cdot)}\tau_{mc}$, it follows that $\tau_{\text{left}} = k_{\text{left}}\tau_{mc}$ and $\tau_{\text{right}} = k_{\text{right}}\tau_{mc}$.

After substituting Eq. (9) into Eq. (27) and careful enumeration, the final expression is

$$\eta_i \pi_i^{q_p} = \begin{cases} (1 - \alpha) \alpha^{i-1+k_{\text{right}}} P_{q_p} \left(P_{f_p} \right)^{m_{lv}+1} \left(I - \alpha^{k_p} P_{f_p} \right)^{-1} \pi^{r_p}, & \text{if } i \leq k_{\text{left}} \\ (1 - \alpha) \alpha^{i-1-k_{\text{left}}} P_{q_p} \left(P_{f_p} \right)^{m_{lv}} \left(I - \alpha^{k_p} P_{f_p} \right)^{-1} \pi^{r_p}, & \text{if } i > k_{\text{left}} \end{cases}, \quad (48)$$

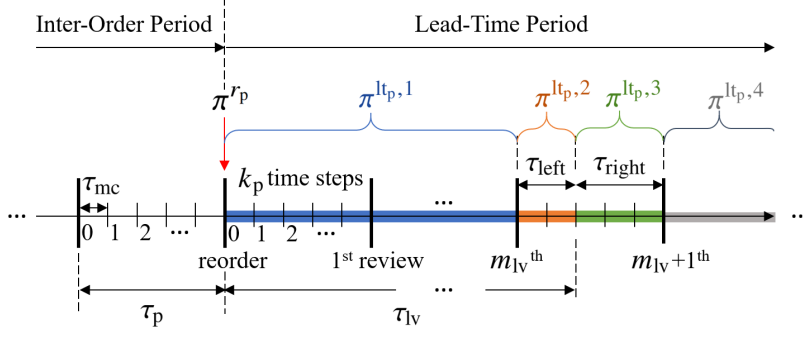


Fig. 8 Timeline with the considered lead-time distribution

where $\alpha = e^{-\tau_{mc}/\mu_{lv}}$, $\forall i = 1, \dots, k_p$. Similarly, the explicit formula for π^{q_p} in Eq. (28) becomes

$$\pi^{q_p} = P_{q_p} \left(P_{f_p} \right)^{m_{lv}} \left((1 - \alpha^{k_{right}})I + (1 - \alpha^{k_p})\alpha^{k_{right}} P_{f_p} \left(I - \alpha^{k_p} P_{f_p} \right)^{-1} \right) \pi^{r_p} \quad (49)$$

Closed-Form Expression for Eq. (32)

As before, we can derive a closed form expression for Eq.(32). Referring to Fig.8, the lead time is divided into four segments, each shown in a different color. The distribution π^{lt_p} is then the weighted sum of the distributions over those four segments. After some algebra and careful enumeration, we obtain

$$\pi^{lt_p} = \frac{1}{k_{lt_p}} \sum_{k=1}^4 \pi^{lt_p,k} \quad (50)$$

where

$$\begin{aligned} \pi^{lt_p,1} &= k_p \left(I + P_{f_p} + \dots + \left(P_{f_p} \right)^{m_{lv}-1} \right) \pi^{r_p} \\ \pi^{lt_p,2} &= (k_{left} + 1) \left(P_{f_p} \right)^{m_{lv}} \pi^{r_p} \\ \pi^{lt_p,3} &= \frac{\alpha \cdot (\alpha^{k_{right}-1} - 1)}{\alpha - 1} \left(P_{f_p} \right)^{m_{lv}} \pi^{r_p} \\ \pi^{lt_p,4} &= \frac{\alpha^{k_{right}} \cdot (\alpha^{k_p} - 1)}{\alpha - 1} \left(P_{f_p} \right)^{m_{lv}+1} \left(I - \alpha^{k_p} P_{f_p} \right)^{-1} \pi^{r_p} \end{aligned} \quad (51)$$

and the unit converted time interval is $\tau_{lt_p} = k_{lt_p} \tau_{mc}$.

The first term, $\pi^{lt_p,1}$, represents the cumulative distribution over the first m_{lv} review cycles, each has k_p time steps. The second term, $\pi^{lt_p,2}$, corresponds to the k_{left} residual steps within the $m_{lv} + 1^{th}$ cycle, during which the distribution remains unchanged. The third and fourth terms, $\pi^{lt_p,3}$ and $\pi^{lt_p,4}$, are derived from a finite and an infinite geometric series, respectively, under the exponential lead-time model.

Closed-Form Expression for Eq. (35)

Here, we derive the closed-form expressions for $\pi^{\text{io}_p|E}$ and $\pi^{\text{lt}_p|E}$ in Eq. (35). During the IO period, RAAN contact always happens at step k_p of each review cycle. Average distribution over these points is actually the second term of Eq. (29) as:

$$\begin{aligned}\pi^{\text{io}_p|E} &= \frac{1}{k_{\text{io}_p|E}} \sum_{j=0}^{\infty} \left(C_{r_p}^+ P_{f_p} \right)^j \pi^{q_p} \\ &= \frac{1}{k_{\text{io}_p|E}} \left(I - C_{r_p}^+ P_{f_p} \right)^{-1} \pi^{q_p},\end{aligned}\tag{52}$$

where $k_{\text{io}_p|E}$ is the normalization constant of $\pi^{\text{io}_p|E}$.

Likewise, during the LT period we apply the same logic to Eq. (32), again evaluating at step k_p . Enumerating all cases for the LT period gives:

$$\begin{aligned}\pi^{\text{lt}_p|E} &= \frac{1}{k_{\text{lt}_p|E}} \left[\sum_{j=1}^{m_{\text{lv}}} \left(P_{f_p} \right)^{j-1} + \sum_{j=0}^{\infty} \rho_{k_{\text{right}}+jk_p}^c \left(P_{f_p} \right)^{m_{\text{lv}}+j} \right] \pi^{r_p} \\ &= \frac{1}{k_{\text{lt}_p|E}} \left[\sum_{j=1}^{m_{\text{lv}}} \left(P_{f_p} \right)^{j-1} + \alpha^{k_{\text{right}}} \left(P_{f_p} \right)^{m_{\text{lv}}} \left(I - \alpha^{k_p} P_{f_p} \right)^{-1} \right] \pi^{r_p}\end{aligned}\tag{53}$$

where $k_{\text{lt}_p|E}$ is the normalization constant of $\pi^{\text{lt}_p|E}$. Referring to Fig. 8, the first term accounts for the cases where E occurs at j^{th} review epoch with $j \leq m_{\text{lv}}$, and the corresponding distribution is $(P_f)^{j-1} \pi^{r_p}$. The second term represents the cases where E occurs at $j > m_{\text{lv}}$, with the probability of still awaiting delivery at that time given by $\rho_{k_{\text{right}}+jk_p}^c$.

Appendix B: Direct Strategy as a Special Case of Parking Policy

The direct strategy is modeled as an (r, q) policy with a shifted exponential lead time distribution [24], while the parking spare policy is modeled as a (r, q, τ) policy with the same lead time model. If the fixed review period becomes the minimum time step (i.e., $k_p = 1$), the demand-induced failure matrix becomes the satellite failure matrix (i.e., $P_{f_p} = P_f$). If both policies share the same (r, q) parameters and the same lead time parameters, they are essentially equivalent by the definition of the (r, q) policy. In this case, we have $k_{\text{left}} = 0$ and $k_{\text{right}} = 1$ from Eq. (47) and as shown in Fig. 8.

Under these conditions, the transition equations between π^q and π^r in Eqs. (25) and (28) become:

$$\begin{aligned}\pi^r &= C_r^- P_f (I - C_r^+ P_f)^{-1} \pi^q, \\ \pi^q &= \sum_{j=0}^{\infty} \rho_{j+1} P_q (P_f)^j \pi^r \\ &= (1 - \alpha) P_q (P_f)^m (I - \alpha P_f)^{-1} \pi^r.\end{aligned}\tag{54}$$

Likewise, the distributions during the IO and LT periods in Eqs. (30) and (32) are:

$$\begin{aligned}
\pi^{\text{io}} &= \frac{1}{k_{\text{io}}} C_r^+ P_f (I - C_r^+ P_f)^{-1} \pi^q, \\
\pi^{\text{lt}} &= \frac{1}{k_{\text{lp}}} \sum_{k=1}^4 \pi^{\text{lp},k} \\
&= \frac{1}{k_{\text{lt}}} \left(\sum_{i=0}^m (P_f)^i + \alpha (P_f)^{m+1} (I - \alpha P_f)^{-1} \right) \pi^r.
\end{aligned} \tag{55}$$

All four expressions exactly match the results presented in [24].

Using the above equations, one can compute π^{rc} and τ_{rc} as described in Sec. III.C.6. With all stationary distributions computed, the cost and resilience metrics of the direct strategy can be obtained by omitting the parking-orbit related terms in Sec. IV (e.g., parking spare holding cost and orbit transfer cost).

Funding Sources

This research was supported by the Advanced Technology R&D Center at Mitsubishi Electric Corporation.

Acknowledgments

The analysis scripts used to generate the results are available at GitHub repository.

References

- [1] McDowell, J., “Starlink Statistics,” <https://planet4589.org/space/con/star/stats.html>, 2025. Accessed: 2025-07-14.
- [2] Space.com, “Starlink satellites: Facts, tracking and impact on astronomy,” <https://www.space.com/spacex-starlink-satellites.html>, 2025. Accessed: 2025-08-07.
- [3] CNBC, “Amazon launches second batch of Kuiper internet satellites, taking on Elon Musk’s Starlink,” <https://www.cnbc.com/2025/06/23/amazon-kuiper-satellites-musk-starlink.html>, 2025. Accessed: 2025-07-14.
- [4] Space.com, “Arianespace to launch new fleet of OneWeb internet satellites tonight. Here’s how to watch.” <https://www.space.com/arianespace-oneweb-5-satellites-launch-webcast>, 2021. Accessed: 2025-07-14.
- [5] Telecoms Tech News, “China launches first satellites for GuoWang constellation,” <https://www.telecomstechnews.com/news/china-launches-first-satellites-guowang-constellation/>, 2024. Accessed: 2025-07-14.
- [6] Pachler, N., del Portillo, I., Crawley, E. F., and Cameron, B. G., “An Updated Comparison of Four Low Earth Orbit Satellite Constellation Systems to Provide Global Broadband,” *2021 IEEE International Conference on Communications Workshops (ICC Workshops)*, 2021, pp. 1–7. <https://doi.org/10.1109/ICCWorkshops50388.2021.9473799>.

- [7] Cornara, S., Beech, T., Belló-Mora, M., and Martinez de Aragon, A., “Satellite constellation launch, deployment, replacement and end-of-life strategies,” *13th Annual AIAA/USU Conference on Small Satellites*, 1999.
- [8] Luu, M. A., and Hastings, D. E., “On-orbit servicing system architectures for proliferated low-earth-orbit constellations,” *Journal of Spacecraft and Rockets*, Vol. 59, No. 6, 2022, pp. 1946–1965.
- [9] American Enterprise Institute, “Moore’s law meets Musk’s law: The underappreciated story of SpaceX and the stunning decline in launch costs,” <https://www.aei.org/articles/moores-law-meet-musks-law-the-underappreciated-story-of-spacex-and-the-stunning-decline-in-launch-costs/>, Accessed: 2025-07-14.
- [10] Cruz, L. A., Porto, V. F., and Nascimento, A. R., “Reliability of Small Satellites: A Review Focused on the Brazilian Context,” *Journal of Aerospace Technology and Management*, Vol. 13, No. Spec. Issue 1, 2021, p. e20210008. <https://doi.org/10.5028/jatm.v13.1322>.
- [11] Dishon, M., and Weiss, G. H., “A Communications Satellite Replenishment Policy,” *Technometrics*, Vol. 8, No. 3, 1966, pp. 399–409.
- [12] Sumter, B. R., “Optimal Replacement Policies for Satellite Constellations,” Master’s thesis, Air Force Institute of Technology, 2003.
- [13] Jakob, P., Shimizu, S., Yoshikawa, S., and Ho, K., “Optimal satellite constellation spare strategy using multi-echelon inventory control,” *Journal of Spacecraft and Rockets*, Vol. 56, No. 5, 2019, pp. 1449–1461.
- [14] Collopy, P., “Assigning value to reliability in satellite constellations,” *AIAA Space 2003 Conference & Exposition*, 2003, p. 6214. <https://doi.org/10.2514/6.2003-6214>.
- [15] Cuhuran, J. J., Jenkins, M. K., and Walters, M. J., “Quantifying and Evaluating the Resilience of Optimized Space Constellations for Fire Detection,” Tech. Rep. AD1055406, Air Force Institute of Technology, 2017.
- [16] Novak, J., and Hastings, D., “Analysis of proliferated low Earth orbit constellation resilience against solar weather radiation effects,” *Acta Astronautica*, Vol. 202, 2023, pp. 292–302.
- [17] Han, S., Noro, T., and Ho, K., “Analysis and Design of Satellite Constellation Spare Strategy Using Markov Chain,” *arXiv preprint arXiv:2408.09250*, 2024.
- [18] Walker, J. G., “Satellite constellations,” *Journal of the British Interplanetary Society*, Vol. 37, 1984, p. 559.
- [19] Prussing, J. E., and Conway, B. A., *Orbital mechanics*, Oxford University Press, USA, 1993.
- [20] Hillier, F. S., and Lieberman, G. J., *Introduction to operations research*, McGraw-Hill, 2015.
- [21] Castet, J.-F., and Saleh, J. H., “Satellite and satellite subsystems reliability: Statistical data analysis and modeling,” *Reliability Engineering & System Safety*, Vol. 94, No. 11, 2009, pp. 1718–1728.

- [22] U.S. Department of Defense, “Fact Sheet: Resilience of Space Capabilities,” , 2011.
- [23] Burch, R., “A Method for Calculation of the Resilience of a Space System,” *MILCOM 2013 - 2013 IEEE Military Communications Conference*, 2013, pp. 1002–1007. <https://doi.org/10.1109/MILCOM.2013.174>.
- [24] Han, S., Grieser, Z., Yoshikawa, S., Noro, T., Suda, T., and Ho, K., “Analysis and Design of Spare Strategy for Large-Scale Satellite Constellation Using Direct Insertion under (r, q) policy,” *arXiv preprint arXiv:2508.XXXXX*, 2025.
- [25] SpaceInsider, “How Much Does It Cost to Launch a Rocket? [By Type & Size],” , 2025. URL <https://spaceinsider.tech/2023/08/16/how-much-does-it-cost-to-launch-a-rocket/>, accessed: 2025-07-11.
- [26] SpaceX, “Smallsat Rideshare Program,” , 2025. URL <https://www.spacex.com/rideshare>, accessed: 2025-07-11.
- [27] Ainvest, “Rocket Lab’s 48-Hour Launch Turnaround: A Strategic Play for Dominance in the SmallSat Launch Market,” , 2025. URL <https://www.ainvest.com/news/rocket-lab-48-hour-launch-turnaround-strategic-play-dominance-smallsat-launch-market-2506/>, accessed: 2025-07-11.
- [28] Spaceflight Now, “Live Coverage: SpaceX to Launch 27 Starlink Satellites on Falcon 9 Rocket from Cape Canaveral,” , 2025. URL <https://spaceflightnow.com/2025/06/27/live-coverage-spacex-to-launch-27-starlink-satellites-on-falcon-9-rocket-from-cape-canaveral-4/>, accessed: 2025-07-11.
- [29] Dubos, G. F., Castet, J.-F., and Saleh, J. H., “Statistical reliability analysis of satellites by mass category: Does spacecraft size matter?” *Acta Astronautica*, Vol. 67, No. 5, 2010, pp. 584–595. <https://doi.org/https://doi.org/10.1016/j.actaastro.2010.04.017>.
- [30] Langer, M., “Reliability assessment and reliability prediction of CubeSats through system level testing and reliability growth modelling,” Ph.D. thesis, Technische Universität München, 2018.
- [31] Jacklin, S. A., “Small-Satellite Mission Failure Rates,” NASA Technical Memorandum NASA/TM-2018-220034, NASA Ames Research Center, Moffett Field, CA, March 2019.